Automotive Science and Engineering, Vol. 12, No. 4, (2022), 4003-4016

Iran University of Science and Technology

Automotive Science and Engineering

Journal Homepage: ase.iust.ac.ir

ISSN: 2008-9899

Model Based Development of Torque Control Drive for Induction Motors for Micro Electric Vehicles

Mohammed Khalifa Al-Alawi1*, Kamyar Nikzadfar2

1* MSc Student, School of Mechanical, Aerospace and Automotive Engineering, Coventry University
2 Associate Professor, School of Mechanical, Aerospace and Automotive Engineering, Coventry University

ARTICLE INFO

Article history:
Received : 21 Aug 2022
Accepted: 5 Nov 2022
Published: 5 Dec 2022

Keywords:
Electric vehicle
Drive technology
Motor control
Iinduction motors
Direct Torque Control
Model based control design

A B S T R A C T

Electric vehicles are attaining significant attention recently and the current legislation is forcing the automotive industry to electrify the productions. Regardless of electric energy accumulation technology, drive technology is one of the vital components of EVs. The motor drive technology has been mainly developed based on the application which required position/velocity control. In automotive application, however, torque control is an important aspect since the drivers have already used to drive the vehicle based on torque control approach in traditional powertrain system. In this article, a model-based approach is employed to develop a controller which can guarantee the precise control of the induction motors torque for a micro electric vehicle (EV) application regardless of operating conditions. The implementation of the control drive was conducted in MATLAB/Simulink environment, followed by Model In the Loop simulation and testing at various test conditions to confirm the robustness of the developed drive. Direct Torque Control (DTC) with optimum voltage vector selection method is employed to control the motor torque that requires fewer power electronics to process its operation and hence lowers the cost of implementation. The result shows the practicality of the designed control system and its ability to track reference torque commands. Vitally, the controlled approach shows fair abilities to control IMs to produce torque at both the motoring and regenerative modes which is a highly important requirement in electrical propulsion powertrains. Furthermore, the controller's response time was within the industrial standard range which confirms its suitability for industrial implementation at low cost. Sensitivity analysis of the effect of change in controller's hysteresis bandwidth on the output torque was conducted.

1.Introduction

UK's total greenhouse gas emissions in 2018 were approximated to be 451 Mt CO2e, featuring transportation as the major accountable sector amongst others, being responsible for nearly 28% of total emissions [1]. These environmental concerns drive the need to implement electrification in the transportation sector in the UK to reduce dependency on fossil fuels and hence reduce emissions. According to the Transport Energy Model developed by Department for Transport, it is projected that replacing a

*Corresponding Author
Email: m.alalawi98@gmail.com
http://doi.org/10.22068/ase.2022.614

[DOI: 10.22068/ase.2022.614]

petrol operating vehicle with an electric vehicle reduces emissions by 67%, emitting only 120 gCO2/km which is significantly lower than petrol and diesel emissions [2]. In line with the Government's projection in decarbonizing the transport sector to achieve the net-zero target; it is essential to solving the practical problems associated with the use of electric vehicles. The shift towards electric vehicles could raise concerns about the overall efficiency of the powertrain system and its rate of response towards a rapid dynamic variation. Therefore, researchers are focused on the development of control drives to control various parameters of electromotor using advanced control strategies that require expensive electronic devices and hence increase expenditure costs for industrial implementation. Various types of EVs have different powertrain architectures; nevertheless, the motor and drive are core technologies that are effective in all EV topologies. Motor and drive are costly; therefore, an optimum cost-benefit ratio should be adopted during the planning phase of control drive design. According to a leading EV drive supplier [3], it is essential to consider a less complicated but simpler design of motor drives to reduce the overall cost of EV powertrain and hence ease the transportation transition to EVs as per the government's projection Similarly, satisfying the requirements for a better performance drive should not compromise the component weight and installation space as these consequences would lead to further expenditure in the manufacturing process of EVs. In the EV industry, motor drives are used to control several parameters of the vehicle's prime mover including torque, speed and rotational shaft position. This is performed using controlling techniques that are software programmed and processed via data processing devices and auxiliary power electronics. This article addresses a major technical uncertainty faced by electric vehicle manufacturers which is the complexity of achieving stable torque control of the electromotor at steady and transient operations. Advanced control strategies are investigated to design an optimal torque controller of the electrical machine to enhance the performance of EV at lower costs. Most high performing drives in the market use field-oriented Control (FOC) since this vector method allows IM dynamics to be represented similar to a separately excited DC motor. However, it requires high-level computational methods and complex mathematical expressions, necessitating powerful processing devices [4]. Furthermore, FOC involves actual rotor position within its computation which necessities feedback devices to be installed, hence increased costs for industrial implementation [5]. Another control technique is known as Direct Torque Control (DTC), is simple to implement and outputs good torque control in transient operation. Nevertheless, there are challenges accompanied with its performance in particular applications including high ripple of torque and flux signals and difficulty in controlling torque at a lower speed range. DTC is characterized by its simple construction providing decoupled control of torque and flux. The technique works by selecting the optimum voltage vector using hysteresis controllers and a voltage source inverter. Since this technique, allows control of both flux and torque an appropriate selection of preference flux is required. An optimization method known as Loss Model Control was described in [6] that leads to generating optimum flux reference value at low load conditions, mitigating increased iron and copper losses. Results obtained from the comparative study aimed to assess the effectiveness of the proposed solution showed that tests with constant reference flux demonstrated better performance at the excitation of motor and similar torque response to the optimized method. Therefore, since this research aims to develop a robust torque controller for EV applications that do not operate at low load conditions and to ensure simplicity of industrial implementation; the proposed solution was not considered. Researchers have addressed other challenges accompanied by the use of conventional DTC controlling schemes in

[DOI: 10.22068/ase.2022.614]

general applications, as summarized in Table 1. Although some of the advancements could lead to enhanced performance of control drive for electromotors, most solutions address issues that do not have a major effect on controlling torque in EV applications. For instance, the solution proposed by [7] solves the variable switching phenomenon however leads to a noticeable surge in stator current. Moreover, other solutions including SVPWM and Feedback Linearization require additional encoders and electronic devices which leads to increased costs of implementation.

Table 1:Summary of major findings of enhancement implemented to conventional DTC.

Advancements	Major Findings
Space Vector Width Modulation [8]	Reduced torque and flux ripple content.
Pulse Width Modulation DTC [7]	Produce constant switching frequency and surge in starting stator current.
DTC with Feedback Linearization [10]	Reduced ripple content and improved transient and dynamic responses.

Based on the findings of previous researchers, implementing a Direct Torque Control scheme with optimum voltage vector selection is a cost-effective method however it yields torque ripple. Therefore, this research will implement DTC to investigate if such drawback could majorly affect the performance of an EV and satisfy the main target of the study which is developing a robust DTC drive that would appropriately control output torque of induction motors for EV applications with minimum electronic devices and lower costs of implementation. Although, industry leaders are currently employing PM motors, however the focus in this paper is to develop a controller for a micro-EV which does not require high power density provided by PM motors. Furthermore, literature fell short in co-simulation of DTC with micro-EV as most papers considered commercial sized vehicles, whereas this paper considers controlling torque of IM powered micro EV powertrain at low cost to ease its employment in sustainable or green cities.

Section 2 of this paper discusses the methodology followed to model the control system and relevant algorithms developed. Section 3 illustrates results obtained via Model-in-the-Loop simulation and testing and discusses major findings. Section 4 concludes the research and lists major findings in accordance to study aims and hypothesis.

2. Model based design

To facilitate a comprehensive evaluation of the chosen control topology and its suitability for EV electromotors; a Model-In-the-Loop simulation approach is used. Modelling of control drive was divided into 3 main sections, namely, induction motor, power electronics and control system. Detailed modelling of IMs has been investigated in relevant references [11] [12] and will not be considered here as modelling of IM and actuator has been carried out based on existing models in MATLB Simulink. Detailed modelling of control system using DTC with optimum vector selection method was conducted as detailed in Section 2.2.

2.1.Controlled Machine

Induction motor pre-defined block in MATLAB Simulink was used as the controlled machine to assess the performance of developed control system. a three phase 3 hp induction motor of squirrel cage type having the characteristics given in Table 2 was considered.

[DOI: 10.22068/ase.2022.614]

Table 2:Induction motor specifications, data taken from Ref. [12].

Parameter Symbol	Value	Unit
Voltage Amplitude	162.6	V
Frequency	50	Hz
Stator Resistance	0.435	Ω
Rotor Resistance	0.816	Ω
Stator Leakage Reactance	0.754	Ω
Rotor Leakage Reactance	0.754	Ω
Mutual Inductance	26.13	Ω
Poles	4	-
Inertia	0.089	$kg.m^2$

2.2.Control System

Control method chosen to model torque control drive is DTC approach which necessitated modelling of Torque and Flux Estimator that acts as a predictive motor model. Additionally, to allow robust control of torque and flux at motoring and regenerative modes; hysteresis controllers were used. Optimum sector and vector algorithm was implemented to feed switching signals to VSI. The high-level control system model is depicted in Figure 1, featuring its connection with other components of the system including motor and power electronics.

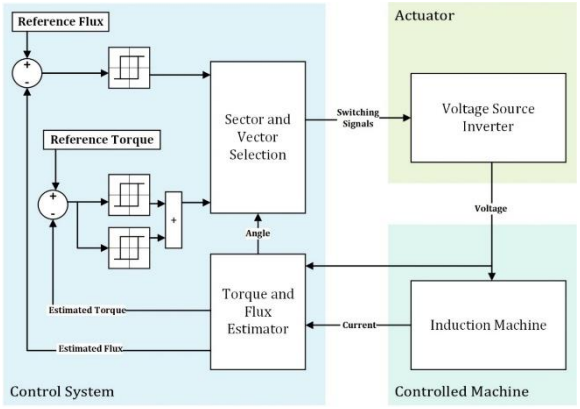

Figure 1:High-level representation of the developed control system model and connections with actuator and controlled machine.

2.2.1.Torque and Flux Estimator

An appropriate stator flux and torque estimation model is required for accurate error calculations to be used for control design. The estimator is an essential component of the control drive as it facilitates control of output torque via its input to a comparator that produces an error signal. Dynamic equations of the motor adaptive model described in [7] and [9] were followed to model the torque and flux estimator illustrated in Figure 2.

2.2.2.Hysteresis Controllers

The process of torque control is conducted by comparing reference torque command and estimated torque, allowing an error signal to be produced as demonstrated in eq. 1. To ensure that the developed controller can increase, decrease or maintain the output torque to match the reference torque

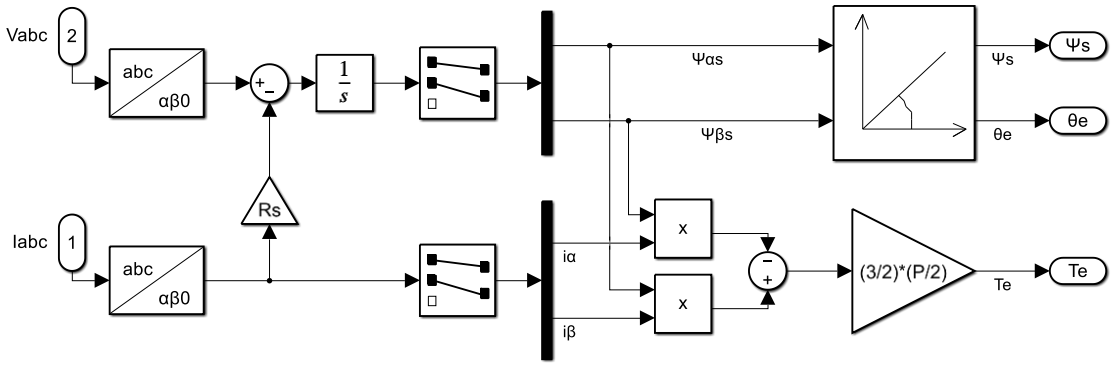

Figure 2:Estimator model developed in MATLAB Simulink environment.

[DOI: 10.22068/ase.2022.614]

command; a three-level hysteresis controller is required. Therefore, two hysteresis relay blocks are required to output three-level digital signals. The possible conditions are stated based on the hysteresis bandwidth or threshold. The condition stated in eq. 2 functions when output torque requires an increment, condition stated in eq. 3 functions when the output torque requires a reduction and condition stated in eq. 4 functions to maintain the output torque. Implementation of these conditions confirms that the controller would be able to control the developed torque at motoring and regenerative modes of the motor.

$$\text{Torque Error} = \mathrm{T_{ref}} - \mathrm{T_{est}} \tag{1}$$

$$\text{Output} = 1, \quad \text{if (Torque Error)} > \text{HB} \tag{2}$$

$$\text{Output} = -1, \quad \text{if (Torque Error)} < -\text{HB} \tag{3}$$

$$\text{Output} = 0, \quad \text{if } -\text{HB} < \text{(Torque Error)} < \text{HB} \tag{4}$$

Similar to torque control, flux control is obtained via a two-level controller that necessitates a single hysteresis relay block to be added to the controller model. Output signals of torque and flux hysteresis controllers are fed to the switching signals generator to select optimum switching states of the actuator.

2.2.3.Switching Signals Generator (Sector and Vector Selection Algorithms)

Generation of appropriate switching signals is based on two main stages as demonstrated in Figure 3, which are the sector selection and vector selection stages. Input to the sector selection is the angle between alpha and beta flux vectors θ_e , which determines the location of stator flux vector in the complex plane.

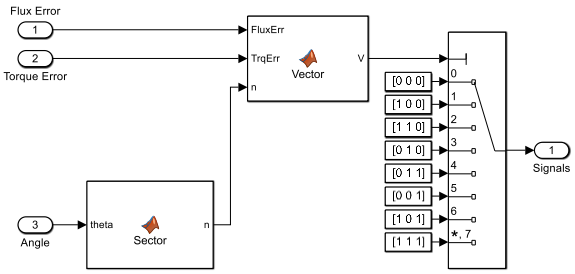

Figure 3:Switching signals generator model developed in MATLAB Simulink Environment.

Figure 4 illustrates the complex plane divided into 6 sectors, where each has an active voltage vector that is placed 60° away from the adjacent vector. Vectors 1 to 6 represent the active states of the VSI, whereas Vector 0 and 7, at the centre of plane, represent null vectors. Implementation of this approach allows to locate the flux vector via the computed flux angle. For instance, if $\theta_e = 40°$ at t=1s, the flux vector will be located at sector 1 and if $\theta_e = 130°$ at t=2s, flux vector will be placed at sector 3.

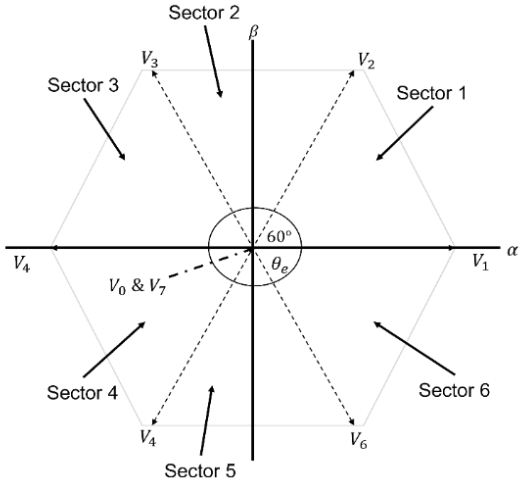

Figure 4:Sector selection of required voltage vector approach, edited from [10].

The other stage of the switching signal generation is the voltage vector selection which requires the following parameters as inputs; namely, stator flux sector (determined from sector selection stage) and torque and flux error signals (obtained from the hysteresis comparators). Dependent on the error signals from the hysteresis controllers; the appropriate voltage vector and hence the switching state will be chosen and fed to the actuator. As shown in the motoring graph, choosing vectors 2 and 3, allow output torque to be increased at sector 1, this concludes that increasing the angle of stator flux vector in

[DOI: 10.22068/ase.2022.614]

the direction of rotation leads to increasing torque and vice versa.

Algorithm flowcharts of sector selection and voltage vector switching techniques, shown in Figure 5 and Figure 6 respectively, were developed and followed to be implemented as MATLAB functions. Algorithm shown in Figure 5 is only for sector 1, however similar approach was followed for other sectors using data found in [7].

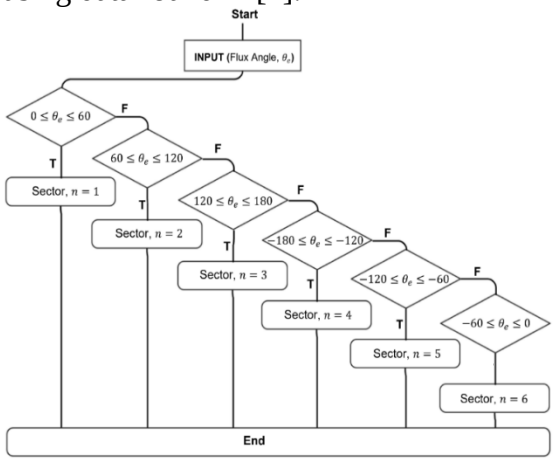

Figure 5:Algorithm flowchart of sector selection technique.

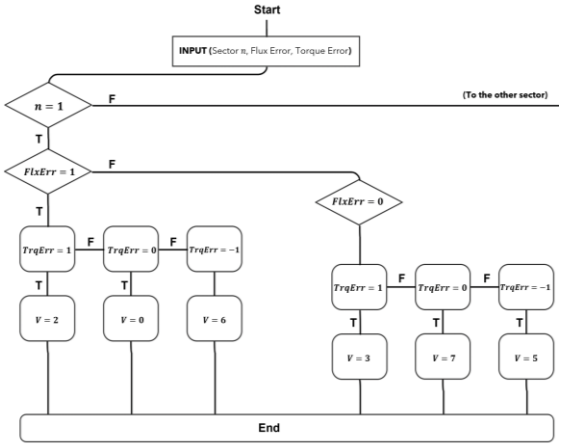

Figure 6:Algorithm flowchart of vector selection technique.

2.3.Actuator

Since the developed control drive is designed to generate switching signals to a VSI it is essential to explore the working principle of the selected VSI. The selected converter for this project is the two level VSI pre-defined block in MATLAB Simulink that consists of six switching devices which operate based on the selected voltage vector as illustrated in Table 3.

Table 3:Switching states of 2-level VSI.

State/Vector	Switching Device 1	Switching Device 2	Switching Device 3
0	0	0	0
1	1	0	0
2	1	1	0
3	0	1	0
4	0	1	1
5	0	0	1
6	1	0	1
7	1	1	1

3. Results and Discussion

Model in The Loop testing technique was used to abstract the behavior of control system within the desired environment. This approach allows testing controller's strategy before running it on real-time hardware which is a highly efficient methodology in industrial applications. Figure 1 demonstrates the configuration of MIL simulation, featuring all components of the control system, actuator and the controlled system (IM). In real practice, reference torque command is produced via a speed controller, however due to the focused scope of this project; torque commands were user defined to perform different testing scenarios. Table 4 provides a summary of inputs and outputs of each component of the MIL configuration. Adjustment of control variables is essential to obtain highest performance of the control drive for the desired response. Therefore, an initial simulation test was conducted to assess the effect of hysteresis bandwidth variation on the controller's response. Figure 7 demonstrates the consequence of reducing HB from 1 to 0.5; as illustrated torque ripple experienced a reduction by half. Therefore, a direct relationship between HB and torque ripple can be concluded, where increasing HB leads to an increase in torque noise.

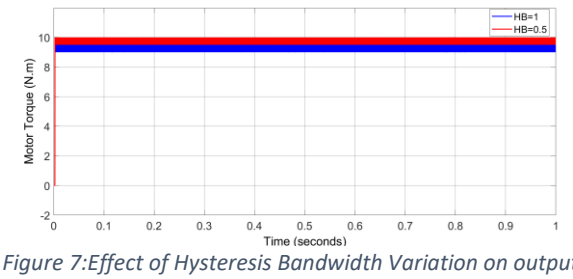

Figure 7:Effect of Hysteresis Bandwidth Variation on output Torque.

[DOI: 10.22068/ase.2022.614]

Hence, controller's tuning is required to obtain the minimum torque ripple possible for a high-performance control drive. Conducted simulation has shown that variation of HB affects the switching frequency per cycle which hence affects the switching time of the control drive. As illustrated in Figure 8, reducing HB results in a significant increase in the switching frequency which could be considered as an industrial drawback as it requires advanced data processing devices.

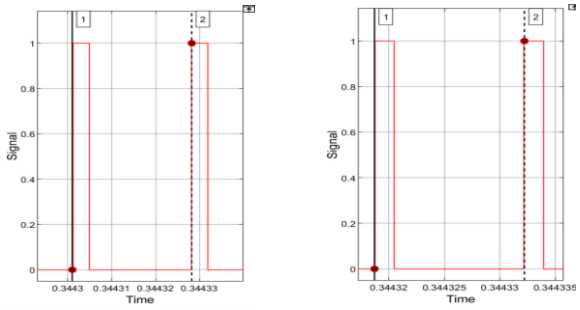

Figure 8:Switching Signals at (a) HB=1 and (b) HB=0.5.

According to [14] 25 µs is an immense processing speed for a torque control drive, in which the VSI switching devices are fed with optimum switching signals leading to powerful torque control. Therefore, to ensure that developed controller is acceptable for industrial implementation, a linear interpretation method was used to estimate the HB value that could produce switching signals with a frequency of 40 kHz, equivalent to pulse time period of 25 µs. The linear interpretation technique featured data illustrated in Figure 8 as the known variables to calculate the required parameter. Results have shown that a HB of 0.918 computes switching signals with a frequency of 39.73 kHz which is within industrial acceptable range and with minimum possible torque ripple.

Different test scenarios with relevance to EV behavior were performed to examine the performance of developed torque control drive via DTC technique with a constant flux reference of 1.1 Wb, DC voltage terminal of 530 V and a constant HB of 0.918. The tests involve different working conditions to examine controller's response towards sudden and dynamic changes, higher torque levels, variations in load torque and EV passive load.

3.1.Constant Reference Torque at Varied Load Conditions

This simulation test was performed to examine the controller's capability of maintaining a persistent output torque despite the variations in load torque. Reference torque command was set to 15 N.m and load torque increases in steps as shown in Figure 10.

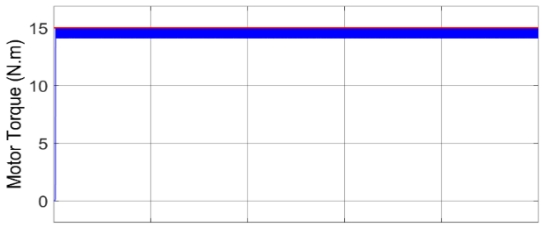

Figure 9:Developed torque result of the constant reference torque test.

As evident, the controller drive showed successful strategy of controlling motor's torque at various load conditions, resulting in a constant output signal as illustrated in Figure 9.

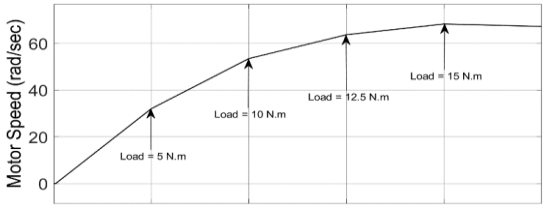

Figure 10:Motor speed at various load conditions.

Remarkably, estimated flux has shown distortion from the required command at t<0.1 s as highlighted in Figure 11. However, for the rest of the simulation, flux signal was maintained at 1.1 Wb as required.

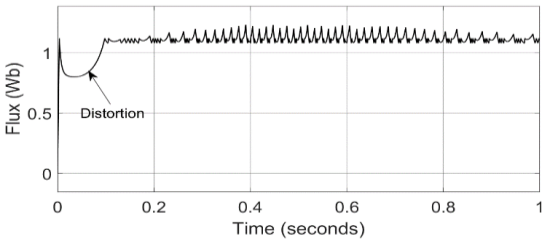

Figure 11:Estimated flux result of the constant reference torque test.

Furthermore, at the initial stage of simulation, surge current was noticed that can be seen in

[DOI: 10.22068/ase.2022.614]

Figure 12. Similarly, a minor ripple was observed in both stator flux and current which was mainly caused by the flux hysteresis controller.

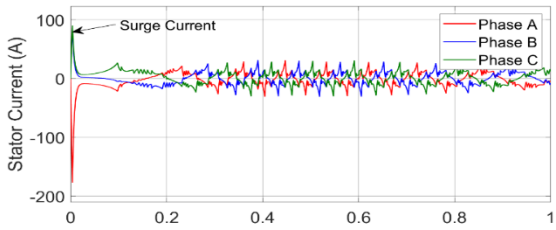

Figure 12:Stator current of the controlled motor.

3.2.Dynamic Loads

This test was conducted to assess the controller's response towards rapid dynamic change in the reference torque command. As shown in the Figure 13 the reference torque was set to a variation of positive and negative values to test the motor's behavior at motoring and regenerative conditions with a load torque of 4 N.m. Results illustrates that the developed controller can control the induction machine to produce the required torque appropriately.

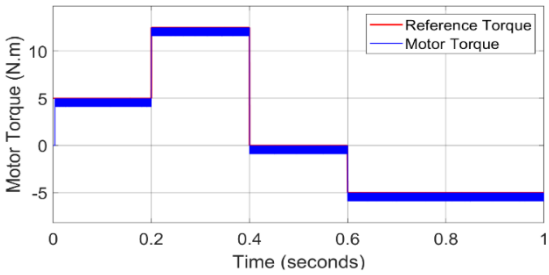

Figure 13:Rapid dynamic variation result, showing developed motor torque against reference.

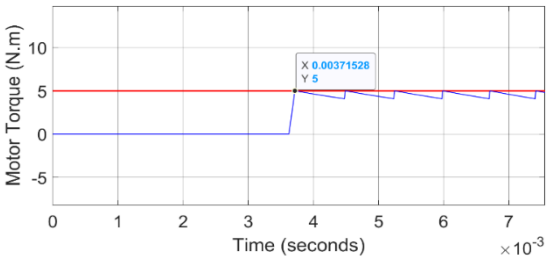

Figure 14:Rapid dynamic variation result zoomed in at t (0 – 0.007s).

3.3.Smoother Dynamic Variation

To replicate the driving behavior of an EV, this test was performed with a smoother variation in reference torque command and with load torque of 4 N.m. Illustration of the result is shown in Figure 15, which confirms that the drive functioned fittingly to requirements at slow variations in torque and steady state condition.

Table4: Summary of inputs and outputs of each system component in MIL configuration

	System	Input	Output(s)
Controlled System	Induction Machine	• Load Torque • 3-Phase Voltage	• Mechanical Torque • Mechanical Speed
Control System	Estimator	• Current and • Voltage Measurement	• Estimated Torque • Estimated Flux
	Hysteresis Controllers	• Reference Torque • Reference Flux • Estimated Torque • Estimated Flux	• Toque Comparator Output • Flux Comparator Output
	Switching Signal Generator	• Toque Comparator Output • Flux Comparator Output • Flux Angle	• Switching Signals
Actuator	2-level Voltage Source Inverter	• Switching Signals	• 3-Phase Voltage

[DOI: 10.22068/ase.2022.614]

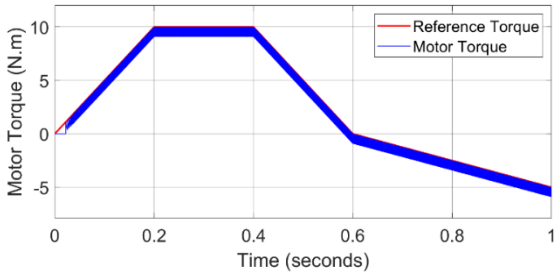

Figure 15:Smooth Dynamic variation simulation result, showing developed torque.

When zoomed in to the initial stage of simulation as in Figure 16 it can be observed that the response was slower and occurred at 22 ms.

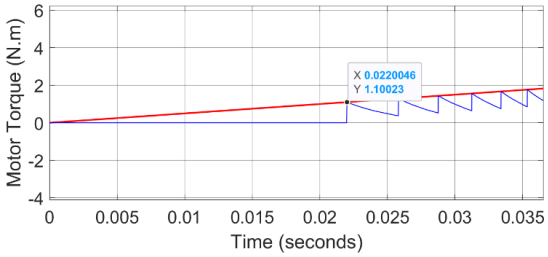

Figure 16: Smooth Dynamic variation simulation result, zoomed in at (0 – 0.035s).

3.4. High Reference Torque

Initial tests have confirmed motor's output torque experience a 0.918 N.m torque ripple due to the hysteresis bandwidth of torque comparators. Therefore, this test was conducted to assess the effect of torque ripple at reference torque command of 130 N.m and load torque of 125 N.m. As demonstrated in Figure 17, when the motor operates at higher torque, torque ripple is hardly noticeable.

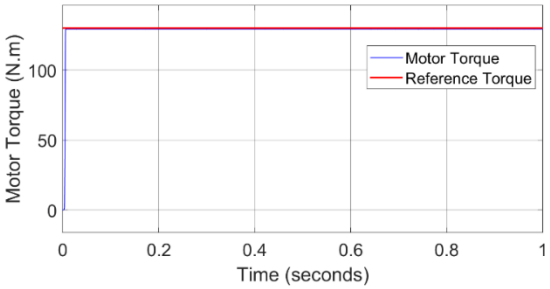

Figure 17: Motor's output torque in comparison to high reference torque command.

3.5.Validation with Passive EV Load

A simulation method was proposed in [13] to analyze the performance of in-wheel electromotor and its auxiliary drives for an electric vehicle which is known as passive loading scheme which reflects vehicle model using forward analysis method. The technique utilizes a simple EV model to extract torque-speed characteristics that can thereafter be used as passive load to the motor. The paper used the technique to achieve torque-speed characteristics of a 200 kg EV with two wheels of equal size. Table 5 was used to develop two look up tables to locate the required torque (reference command) and wheel speed (load) based on vehicle speed. Driving cycle, NYCC, available in Simulink was used as the input to both look up tables.

Table5: Steady state vehicle and wheel speed for a constant applied torque, Data taken from Ref. [13].

Torque (N.m)	Steady State Vehicle Speed (Km/h)	Steady State Wheel Speed (rpm)
10	25	241
20	36	342
30	44	418
40	51	483
50	57	540
60	62	592
70	67	639
80	72	783
90	76	725
100	80	764

Simulation was run for entire driving cycle duration, 598s, to examine the controller's behavior in a real driving cycle and for a longer time. As illustrated Figure 18, the output torque is tracking the driving cycle appropriately with no major distortions. A minor signal distortion is noticed when a

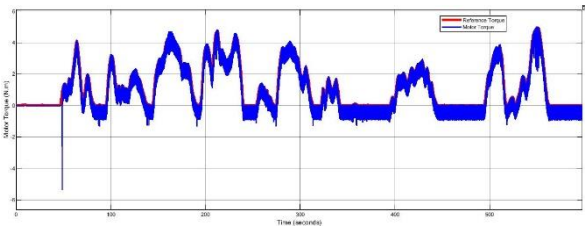

Figure 18:Motor torque behavior for 598 seconds of NYCC driving cycle.

[DOI: 10.22068/ase.2022.614]

Table 6. Torque hysteresis limit values.

		Torque Hysteresis Upper Limit		
		HB = 0.918	75% HB = 0.6885	50% HB = 0.459
Torque Hysteresis Lower Limit	HB = (-0.918)	Figure 19	Figure 23	Figure 26
	75% HB = (-0.6885)	Figure 20	Figure 22	Figure 27
	50% HB = (-0.459)	Figure 21	Figure 24	Figure 25

transition from steady to transient condition has occurred.

3.5.1. Sensitivity Analysis

A sensitivity analysis was conducted to the validation with EV passive Load to assess the effect of HB on the output-controlled torque. Simulation was repeated with varied hysteresis bandwidth values as in Table 6 with NYCC driving cycle as input command and ran for 100s.

Results of sensitivity analysis demonstrate the effect of varying HB on the output work. when lower HB limit was set to 75% of original HB, initial distortion when transitioning from steady to transient condition was significantly reduced as illustrated in Figure 20 in contrast to Figure 19. Figure 25, Figure 26 and Figure 27 confirm that when upper HB limit was set to 0.459, torque ripple was lowered in contrast

to performance of 75% and 100% HB controllers and the undesirable initial distortion was mitigated. However, selecting a lower HB value would increase switching frequency of the drive and hence requires high power processers of higher costs. Therefore, tjorough analysis shall be conducted to select appropriate HB to obtain a robust control drive with compatiable processors.

Table 7. Major findings of MIL tests conducted.

Simulation Test	Finding(s)
3.1	• Persistent output torque maintained. • Mitigate the effect of variable load torque. • Drop in flux signal and surge in current at initial stage of simulation.
3.2	• No distortion noticed at time of rapid variation. • Provided appropriate control of output torque. • Fast response time (3.7 ms). • Optimum performance at motoring and regeneration.
3.3	• Excellent tracking of reference torque signal. • Response time (22 ms).
3.4	• Torque ripple had no effect on the output torque. • Torque ripple hardly noticeable.
3.5	• Tracked the driving cycle fittingly with no major distortions for 598 s. • Performed well at forward and braking conditions. • Constant low ripple of 0.918 N.m maintained. • Minor distortion at initial excitation of vehicle.

[DOI: 10.22068/ase.2022.614]

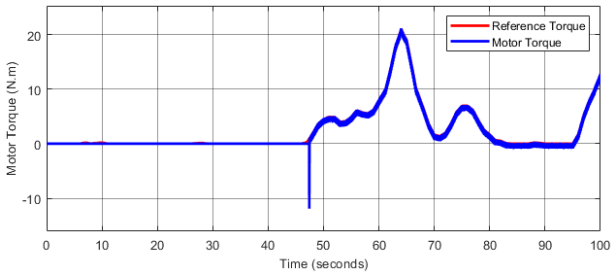

Figure 25: Upper and Lower limits of Torque Hysteresis controllers are set to 0.918 and (-0.918) respectively.

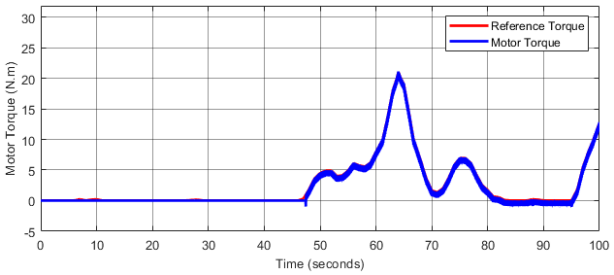

Figure 24: Upper and Lower limits of Torque Hysteresis controllers are set to 0.918 and (-0.6885) respectively.

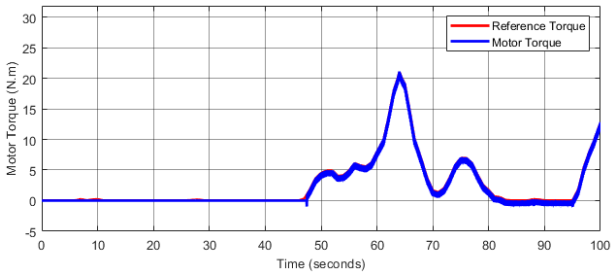

Figure 23: Upper and Lower limits of Torque Hysteresis controllers are set to 0.918 and (-0.459) respectively.

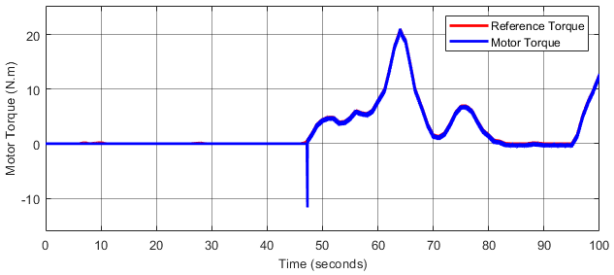

Figure 22: Upper and Lower limits of Torque Hysteresis controllers are set to 0.6885 and (-0.6885) respectively.

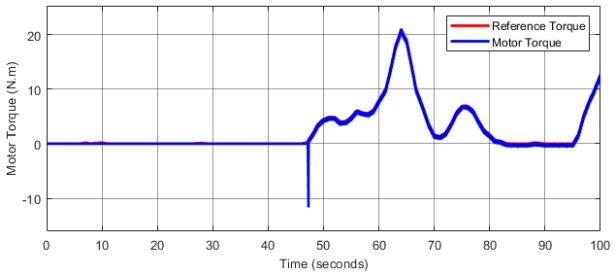

Figure 21: Upper and Lower limits of Torque Hysteresis controllers are set to 0.6885 and (-0.918) respectively.

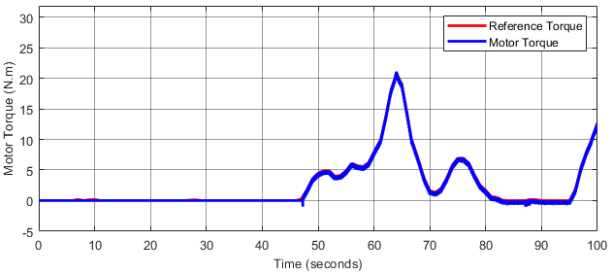

Figure 20: Upper and Lower limits of Torque Hysteresis controllers are set to 0.6885 and (-0.459) respectively.

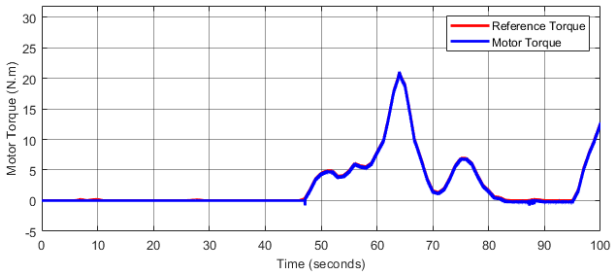

Figure 27: Upper and Lower limits of Torque Hysteresis controllers are set to 0.459 and (-0.459) respectively.

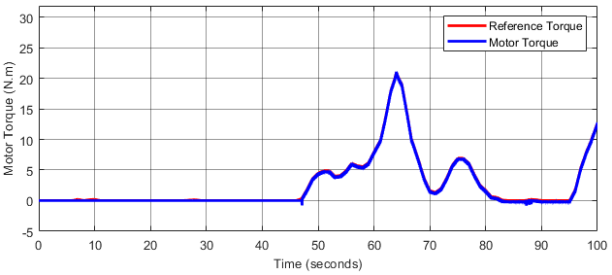

Figure 26: Upper and Lower limits of Torque Hysteresis controllers are set to 0.459 and (-0.918) respectively.

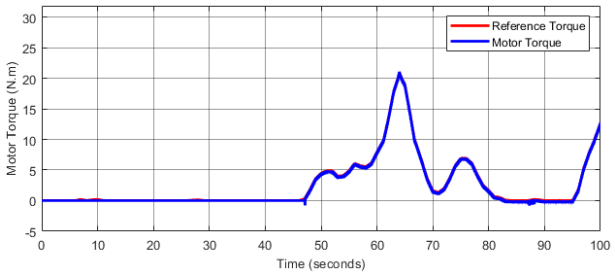

Figure 19: Upper and Lower limits of Torque Hysteresis controllers are set to 0.459 and (-0.6885) respectively.

[DOI: 10.22068/ase.2022.614]

Based on obtained results of MIL testing, summarized in Results of sensitivity analysis demonstrate the effect of varying HB on the output work. when lower HB limit was set to 75% of original HB, initial distortion when transitioning from steady to transient condition was significantly reduced as illustrated in Figure 20 in contrast to Figure 19. Figure 25, Figure 26 and Figure 27 confirm that when upper HB limit was set to 0.459, torque ripple was lowered in contrast to performance of 75% and 100% HB controllers and the undesirable initial distortion was mitigated. However, selecting a lower HB value would increase switching frequency of the drive and hence requires high power processers of higher costs. Therefore, tjorough analysis shall be conducted to select appropriate HB to obtain a robust control drive with compatiable processors.

Table 7; the developed torque control drive using DTC scheme has shown excellent performance in controlling torque for automotive applications. It has a fast response time of 3.7 ms which is within industry acceptable range; as according to drive technical guidelines prepared by [14], efficient torque drives respond within 5 ms. Nevertheless, results of smooth variation in required torque demonstrated a response time of 22 ms. Delay in response was experienced because commanded reference torque signal starts from 0 N.m and in accordance with the threshold set to torque hysteresis switch; it only functions when there is an error signal of 0.918 N.m or above. Such latency is not considered a drawback since EV do not operate at very low torque levels.

Estimated flux waveform was constant throughout simulation tests since the reference flux command was set to 1.1 Wb; this confirms that one of the essential targets of implementing DTC method which is decoupling of torque and flux and hence acquiring separate control of both. However, a noticeable fall in flux signal was noticed which could be due to the unfavorable transient occurring at the excitation of IM such as inrush current, such action is considered unhealthy and could lead to failure of the VSI. A solution proposed by [7] states that poor transients occurring at the excitation of motor can be solved by implementing an algorithm to the speed controller which is responsible of producing torque commands. However, this solution was not implemented in this study because configuration of MIL followed does not involve use of speed controller, instead direct reference torque signals are commanded.

Conducted tests have confirmed controller's robustness in controlling torque of IM; however, since the study focuses on achieving torque control of IM powered EVs, it is essential to evaluate produced torque ripple on higher torque levels. Drive was experimented to control IM at reference torque of 130 N.m and remarkably there was no distortion observed and a constant 0.918 N.m ripple was maintained. Torque ripple experienced is insignificant and would not cause discomfort to vehicle passenger, particularly that it equates to 0.7% of the operating torque. Furthermore, in EV application, yielding higher inertial load; sudden changes in torque would not result in rapid variation of speed and acceleration. Inertia of an EV plays an essential role on deciding acceptable noise in developed torque; therefore, EV passive load was conducted. Common control approach employed in EVs is speed control which has a different driving habit in contrast to ICE propelled vehicles; DTC methodology allows EV to hold drivability similar to ICE vehicles. Results have shown that with an appropriate driving cycle, designed controller was able to effectively track desired behavior. Consistently, the controller was able to mitigate torque forwarding and braking variations caused by the driving cycle. Nevertheless, a minor distortion was noticed when the vehicle moved from steady state to transient condition and this could be due to unfavorable inrush current.

[DOI: 10.22068/ase.2022.614]

4.Conclusion

In conclusion, a powerful and robust model-based torque drive was developed to control the mechanical torque of an induction machine at both motoring and regenerative modes. Suitability of the controller to be used for EV applications has been confirmed via Model-In-the-Loop simulation and testing under various test scenarios. Results have confirmed the controller's ability to perform the following:

- Maintains constant torque output despite the change in load torque levels.
- Provides superb control of torque and flux separately.
- Tracks positive and negative reference torque commands (motoring and regenerative modes).
- Fast response to sudden changes in torque levels.
- Maintained minimal torque ripple at higher torque levels.
- Control an IM with EV load appropriately at forward and braking conditions.

Therefore, this study has confirmed that the torque ripple caused by conventional DTC scheme are not relevant for EV applications due to their working principle Furthermore, it was also concluded that it is essential to evaluate the advances in controlling principles as they require additional power electronics and increased costs to solve problems thar are not major for a particular application, EV in this study. However, such advances could be very essential in applications that operate at lower torque levels, hence the torque ripple could cause major issues, for instance in robotics. The study has satisfied the predetermined aims and succeeded in developing a robust torque control drive of induction motors for EV applications using simple topologies and reduced costs if implemented.

References

[1].Department for Business, Energy and Industrial Strategy. UK Energy In Brief 2020. UK Government, 2021.

[2].Department of Transport. Transport Energy Model Report. UK Government, 2018.

[3].Bosch. The Electric Drive: efficient, dynamic, and with zero local CO2 emissions. 2021.

[4]. Jisha, L.; Thomas, A.P. A comparative study on scalar and vector control of Induction motor drives. Proceedings of 2013 International conference on Circuits, Controls and Communications (CCUBE), Bengaluru, India, 27-28 December 2013. IEEE: 2013. DOI: 10.1109/CCUBE.2013.6718554

[5]. Deshmukh, S..; Tiwari, N. ANN based DTC for Induction Motor Drive. IJERT 2014, 3, 1040-1044. DOI:

[6]. Ammar, A.; Benakcha, A.; Bourek, A. Closed Loop Torque SVM-DTC based on Robust Super Twisting Speed Controller of Induction Motor Drive with Efficiency Optimization. IJHYDENE 2017, 42, 17940-17952. DOI: 10.1016/j.ijhydene.2017.04.034.

[7]. Brandstetter, P.; Kuchar, M.; Vo, H.H.; Dong, C.S. Induction motor drive with PWM direct torque control. Proceedings of 18th International Scientific Conference on Electric Power Engineering (EPE), International conference on Circuits, Controls and Communications (CCUBE), Kouty nad Desnou, Czech Republic, 17-19 May 2017. IEEE: 2017. DOI: 10.1109/EPE.2017.7967268.

[8].Laskody, T.; Dobrucky, B.; Kascak, S.; Prazenica, M. 2-phase direct torque-controlled IM drive using SVPWM with torque ripple reduction: Motoring and regenerating. Proceedings of 23rd International Symposium on Industrial Electronics (ISIE), Istanbul, Turkey, 1-4 June 2014. IEEE: 2014. DOI: 10.1109/ISIE.2014.6864697.

[9].Raj, A.; Sharma, R. Improved Direct Torque Control for Induction Motor in Electric Vehicle

[DOI: 10.22068/ase.2022.614]

Application. Proceedings of 8th I Power India International Conference (PIICON), Kurukshetra, India, 10-12 December 2018. IEEE: 2018. DOI: 10.1109/POWERI.2018.8704469.

[10]. Muddineni, V.P.; Sandepudi, R.S.; Bonala, A.K. Simplified finite control set model predictive control for induction motor drive without weighting factors. Proceedings of International Conference on Power Electronics, Drives and Energy Systems (PEDES), Trivandrum, India, 14-17 December 2016. IEEE: 2016. DOI: 10.1109/PEDES.2016.7914258.

[11]. Kim, S. H. (2018) Electric Motor Control: DC AC and BLDC Motors. Amsterdam: Elsevier.

[12]. Rai, T.; Debre, P. Generalized modeling model of three phase induction motor. Proceedings of International Conference on Energy Efficient Technologies for Sustainability (ICEETS), Nagercoil, India, 7-8 April 2016. IEEE: 2016. DOI: 10.1109/ICEETS.2016.7583881.

[13].Makwana, J.A.; Agarwal, P.; Srivastava, S.K. Novel simulation approach to analyses the performance of in-wheel SRM for an Electrical Vehicle. International Conference on Energy, Automation and Signal (ICEAS), Bhubaneswar, India, 28-30 December 2011. IEEE. DOI: 10.1109/ICEAS.2011.6147103.

[14]. ABB. Technical guide No. 1: Direct torque control – the world's most advanced AC drive technology. ABB, 2011.

[DOI: 10.22068/ase.2022.614]